RSC Advances


Volume 1 | Number 1 | Jan 2013 | Pages 1–100

RSC Advances

www.rsc.org/advances

ROYAL SOCIETY
OF CHEMISTRY

www.rsc.org/advances

Graphical abstract

Nylon-6/POMs composite nanofibrous membranes were fabricated by electrospinning technique, which show good degradation property toward HD and high filtration performance.

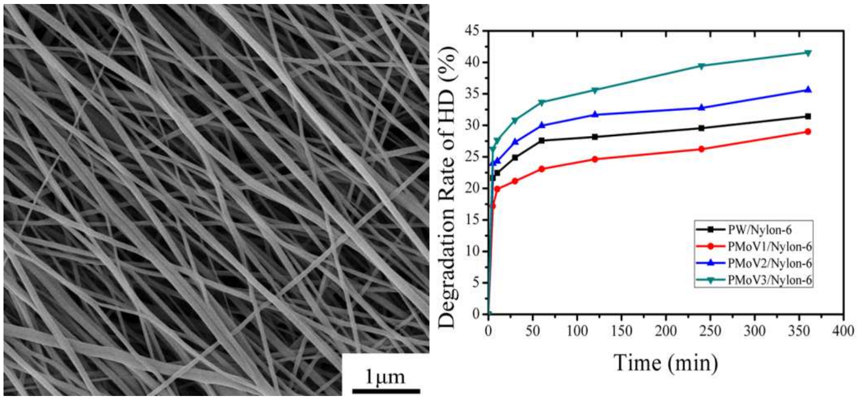

Fabrication of Nylon-6/POMs nanofibrous membranes and the degradation mustard stimulant research

Feng Liu,[a] Qifang Lu,[b] Xiuling Jiao[a,]* and Dairong Chen[a,]*

[a]School of Chemistry & Chemical Engineering, National Engineering Research Center for Colloidal Materials, Shandong University, Jinan 250100, P. R. China.

[b]Shandong Provincial Key Laboratory of Processing and Testing Technology of Glass & Functional Ceramics, Qilu University of Technology, Jinan 250353, P. R. China.

Four kinds of Nylon-6/POMs ($H_{3+n}PMo_{12-n}V_nO_{40}\cdot xH_2O$ and $H_3PW_{12}O_{40}\cdot xH_2O$) composite nanofibrous membranes were fabricated by electrospinning the mixed solution of nylon-6 and POMs using HCOOH and water as solvents. The membranes were composed of randomly arranged Nylon-6/POMs composite nanofibers with diameter range from 50 to 100 nm. Thermal gravimetric (TG) and differential scanning calorimetric (DSC) characterization indicates high thermal stability of the membranes. The degradation ability of the composite fibrous membranes toward mustard (HD) was investigated. The results showed that the membrane has a good degradation performance toward HD with the degradation percentage as high as 41.55%. Degradation rates of HD by the four kinds of nanofibrous membranes are in the order of PMoV3/Nylon-6>PMoV2/Nylon-6>PW/Nylon-6>PMoV1/Nylon-6. At the same time, the nanofibrous membrane exhibit good filtration performance toward aerosol. The fabricated composite nanofibrous membranes show potential application in the in situ degradation of HD, and may be applied as a protecting cloth.

---

* Corresponding author. E-mail address: jiaoxl@sdu.edu.cn. Tel: +86-531-88364280. Fax: +86-531-88364280.

1. Introduction

Chemical warfare agents are used for war purpose with toxic effects on humans and animals as the main means of destruction of chemical substances.[1-3] As a typical erosive chemical warfare agent, mustard (HD) is a blistering agent that attacks the mucous membranes and is lethal at high doses, and there are no specific treatment methods till now. Because of the high toxicity and persistency, HD always plays an important role in the chemical arsenal of many countries since it was firstly used in World War I.[4] Therefore, the detoxification of HD has been intensively investigated in recent years, aimed at eliminating the hazard of HD not only on battlefield but also during its production and storage.[5] Normally, the detoxification of HD is realized by the chemical reaction between detoxicant and HD. In application, the detoxicant solution was firstly prepared, then the contaminated materials were immersed in the solution and reacted under the designed condition for a period of time. The fabrication of novel materials to realize the in situ degradation of HD still remains great challenge.

Polyoxometalates (POMs) are a large class of metal oxide cluster compounds composed of d^0 transition metal atoms, typically W(VI), V(V), Mo(VI), Nb(V) and Ta(V), bridged by oxygen atoms.[5-10] In recent years, polyoxometalates (POMs) have been a category of fast developing oxidative catalysts in organic synthesis and environmental remediation.[11-16] In addition, many types of POMs can change the color when they are reduced.[17] If a chemical warfare agent (CWA), such as HD, contacts with the POM, it would be oxidized and the POM would be reduced with the color changed.[18-20] Therefore, POMs can be applied as detoxicant and indicator of HD simultaneously. For practical application, the load of POMs is a key point, which has aroused great interests in recent years. In previous reports, the researches mainly focused on the combination of

POMs with inorganic nanomaterials[21,22] such as TiO_2,[16,23] which can be used as the photocatalyst. Besides, POMs loaded zeolite,[24] activated carbon,[5,25] and activated carbon fibers[26,27] were also studied. However, most of the reported POMs were loaded on supporting materials by using immersion method, the POMs easily departed from the supporting material due to the poor binding force.[28] Moreover, for these materials, it is difficult to realize the in situ detoxication of HD.

Electrospinning is widely accepted as a technique to fabricate polymer fibers and their membranes.[29,30] Electrospinning is unique as a fiber spinning process because it can consistently generate the polymer fibers ranging from 50 to 500 nm in diameter.[31] Several polymer nanofiber membranes or their composite ones were prepared, which exhibited outstanding properties in the fields of filtration, adsorption, energy, medicine and environment protection. However, there are no reports on the electrospun nanofiber membranes for the detoxication of chemical warfare agents. Therefore, the design and fabrication of electrospun nanofibrous membrane with dual-function of filtration and degradation toward HD is of great importance.

Nylon-6 is a biodegradable and biocompatible polymer with many advantages,[32] and nylon-6 nanofiber membrane has been prepared through electrospinning in previous report.[33] Here, using nylon-6 as the supporting material, we designed and fabricated nylon-6/POMs composite nanofibrous membranes through electrospinning the mixed solution of nylon-6 and POMs, and investigated their detoxication property toward HD. The results indicate that the membranes have good flexibility, high thermal stability, as well as good filtration and detoxication property toward HD. Therefore, the prepared Nylon-6/POMs composite nanofiber membranes are hoped to be applied as materials for protective clothing with in situ detoxication property to HD.

2. Experimental section

2.1. Materials

The starting materials include the polycaprolactam (Nylon-6, Sigma-Aldrich), molybdenum trioxide (MoO_3, Shanghai Chemical Reagent Co. Ltd.), phosphate (H_3PO_4, AR, 85%, Kang De Chemical Co, Ltd., Laiyang), phosphotungstic acid ($H_3PW_{12}O_{40}\cdot xH_2O$, Sinopharm chemical reagent Co.) and vanadium pentoxide (V_2O_5, 95%, industrial grade). Formic acid (HCOOH, AR, 85%, Tianjin Ke Mi Ou Chemical Reagent Co. Ltd.) was used as solvent to dissolve the polycaprolactam. Deionized water with a resistance of 18.2 MΩ was used to dissolve POMs.

2.2. Preparation of $H_{3+n}PMo_{12-n}V_nO_{40}\cdot xH_2O$

Take the preparation of $H_4PMo_{11}VO_4\cdot xH_2O$ for example, 14.4 g of MoO_3 and 0.91 g of V_2O_5 were dispersed in 250 mL deionized water, and then the mixture was heated to 373 K under vigorous stirring, followed by dropwise addition of 1.15 g of phosphoric acid (85 wt%) and kept at 373 K for 24 h. During this process, the slurry gradually became orange transparent solution. After then, the solution was heated in a vacuum oven at a temperature of 327 K to remove the water slowly and the orange-red solid was obtained. Finally, the solid was dissolved in a small amount of deionized water and recrystallized at room temperature three times to obtain pure $H_4PMo_{11}VO_{40}\cdot xH_2O$. The syntheses of $H_5PMo_{10}V_2O_{40}\cdot xH_2O$ and $H_6PMo_9V_3O_{40}\cdot xH_2O$ were similar to that of $H_4PMo_{11}VO_{40}\cdot xH_2O$ with different amount of raw materials.

2.3. Electrospinning preparation of Nylon-6/POMs nanofiber membranes

2 g of nylon-6 was added into 11.3 g of HCOOH, the mixture was stirred for 5 h until the transparent solution was formed. 0.25 g of as-prepared POMs or commercial phosphotungstic acid ($H_3PW_{12}O_{40}\cdot xH_2O$) was dissolved in 2 mL deionized water to form a solution, which was added dropwise into the nylon-6 solution under vigorous stirring to form a transparent orange-red

solution, in which the concentration of nylon-6 was ca.13 wt%.

Nanospider (Elmarco) was used for electrospinning using linear electrode as spinning electrode and cylindrical electrode as collector electrode (Fig. 1). The solution was transferred into the reservoir to make solution contact with the linear electrode. All the fibrous membranes were spun at 60 kV, and the distance between spinning electrode and collector electrode was 18 cm. Polypropylene nonwoven fabric was used as a receiver. The fibrous membranes were peeled from the polypropylene nonwoven fabric and dried at 60 °C for 24 h to remove the solvent completely.

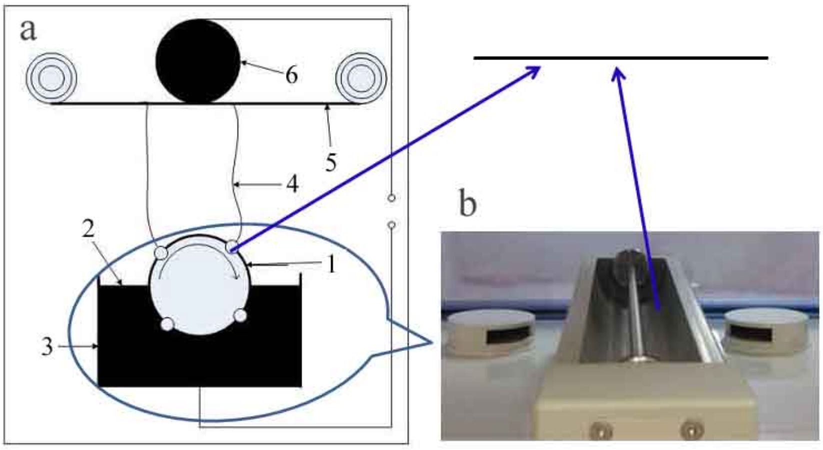

Fig. 1 (a) Illustration of Nanospider used. Legend: (1) linear electrode, (2) polymer solution, (3) solution reservoir, (4) nanofiber, (5) support material, (6) collector electrode. (b) Optical photos of Nanospider used.

2.4. Characterization

Thermal stability of the fibrous membranes was studied by the thermal gravimetric and differential scanning calorimetric (TG-DSC) analyses (Mettler Toledo, TGA/SDTA851e) in air atmosphere at a heating rate of 10 °C/min from room temperature to 800 °C. The FT-IR spectra of the samples were recorded on a Nicolet 5DX-FTIR spectrometer using KBr pellet method in the range of 600-1800 cm^{-1}. The morphology and microstructure of the samples were characterized using the scanning electron microscope (SEM, SUPRA^{TM}55). Chemical compositions of POMs were determined by X-ray fluorescence spectrometer (XRF, S4-explorer). The dichloromethane extracts in the degradation experiments were analyzed by GC-MS (ThermoFinigan DSQ GC-MS under EI conditions: 70 eV, 230 °C) using a 30 m × 0.25 mm ID J&W DB-1MS capillary column and the following temperature program: 40 °C (2 min hold) to 280 °C (5 min hold) @10 °C/min. All injections (1 μL) were cooled on-column at 43 °C. The mass spectrometer was scanned from 40 to 400 Da.

The filtration efficiency and pressure drop were tested on a TSI model 8130 automated filter tester (TSI, Inc., MN, USA), which could deliver charge neutralized oily DOP (Di-Octyl Phthalate) aerosols with a mass median diameter of 330 nm and a geometric standard deviation not exceeding 1.6. The DOP aerosol rate was fixed at 5.3 $cm \cdot s^{-1}$. To meet the requirement of the filtration, a piece of PP nonwoven fabric was used as substrate to receive and support the Nylon-6/POMs nanofibrous membrane.

2.5. Degradation performance of Nylon-6/POMs nanofiber membranes toward HD

Standard solution of HD was prepared. 100 μL HD was diluted with CH_2Cl_2 in a 100 mL volumetric flask to obtain HD standard solution (1 μL (HD)/ mL (CH_2Cl_2)).

Firstly, 150 mg of nanofiber membrane was dipped in 5 mL HD standard solution in a 10 mL flask. After being shocked fully, the flask was kept at 25 °C to start the degradation reaction under stirring. The products were identified by GC-MS at different intervals, such as 10 min, 20 min, 30 min, 60 min, 120 min, 180min, 300 min, 360 min, to track the degradation of HD. At the same time, the experiment without nanofiber membrane was conducted as reference. Each sample was tested three times to give information on reproducibility and obtain accurate results.

3. Results and discussion

X-ray fluorescence (XRF) spectrometry is used for quantitative analysis of the metallic elemental contents in POMs. Table 1 shows the results of XRF. Keggin units have one central atom, 12 transition metal atoms and an appropriate number of charge balancing protons or cations. The Mo/P ratios in as-prepared PMoV1, PMoV2 and PMoV3 are 10.8, 10.3 and 10.0, and the corresponding V/P ratios in these samples are 1.15, 2.12 and 2.94, respectively. Overall, the Mo/P and V/P ratios in these samples are close to those in polyoxometalates $H_{3+n}PMo_{12-n}V_nO_{40}$ (n=1～3) in theory. This indicates that the synthesis method is feasible. At the same time, it is also noted that with the increase in the proportion of vanadium polyoxometalates, the difference between the Mo/P ratio of the sample and the theoretical value increased gradually. It may be related with the stability decrease of the secondary structure in polyoxometalates along with the increase of the relative content of vanadium species.[34]

Table 1 Elemental analysis for PMoVn

Polyoxometalate	Mass fraction (%)			Molar ratio (in sample)		Molar ratio (in theory)	
	P_2O_5	V_2O_5	MoO_3	Mo/P	V/P	Mo/P	V/P
PMoV1	3.55	5.32	77.41	10.8	1.15	11	1
PMoV2	3.53	9.53	73.89	10.3	2.12	10	2
PMoV3	3.44	12.97	70.15	10.0	2.94	9	3

Based on previous studies, FTIR is considered to be a powerful tool to characterize the polyoxometalates. As shown in Fig. 2, there are four distinct characteristic peaks in the wavenumbers range of 1100-700 cm^{-1}, indicating the Keggin structure of the prepared POMs. The peak appearing at 1080-1060 cm^{-1} is ascribed to the P-O stretching vibration. The absorption at ca. 960 cm^{-1} is due to the stretching vibrations of Mo=O bonds. The bands appeared at 860-900 cm^{-1}

and ca. 780 cm^{-1} correspond to the vibrations of Mo-O-Mo, which is significantly influenced by the substitution of Mo by V.[35] As for the phosphotungstic acid ($H_3PW_{12}O_{40}\cdot xH_2O$), the absorption at 1080 cm^{-1} is due to the stretching vibration of P-O bond, and that at 983 cm^{-1} can be ascribed to W=O stretching vibrations. The vibrations of W-O-W appear at 891 and 804 cm^{-1}. Except the vibrations at 1100-700 cm^{-1}, the broad band at ca.1600 cm^{-1} can be observed for POMs including PMoV2, PMoV3 and PW, which is due to the presence of crystallization water. The disappear of this peak for PMoV1 indicates the crystallization water in the sample is removed during the recrystallization process.[35] The IR spectra indicate the Keggin structure of the prepared POMs and commercial PW, and the water in PMoV1 is easily removed comparing to others.

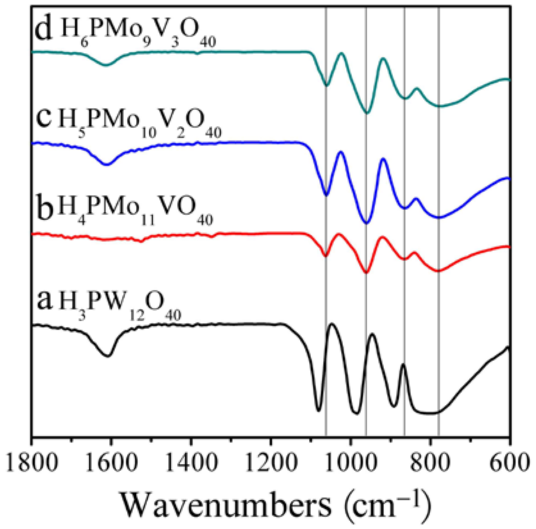

Fig. 2 FTIR spectra of four kinds of POMs.

Phase structure of the prepared POMs was further characterized by XRD technique. Fig. 3 shows XRD patterns of four samples. The strong characteristic peaks at 2θ values of 8~10 °, 16~23 °, 25~30 ° and 31~38 ° were assigned to Keggin structure, which are accordance to the triclinic keggin structure POM (JCPDS No.43-0317). These characteristic peaks were observed in all the samples. The XRD patterns of the four samples (Fig. 3) further indicate the keggin structure of the prepared POMs.

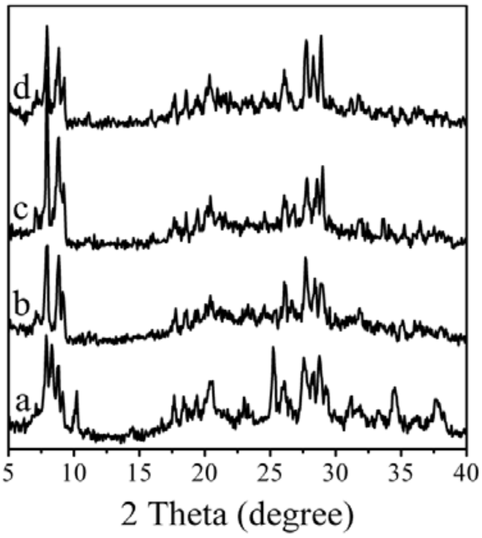

Fig. 3 XRD patterns of (a) PW, (b) PMoV1, (c) PMoV2, (d) PMoV3.

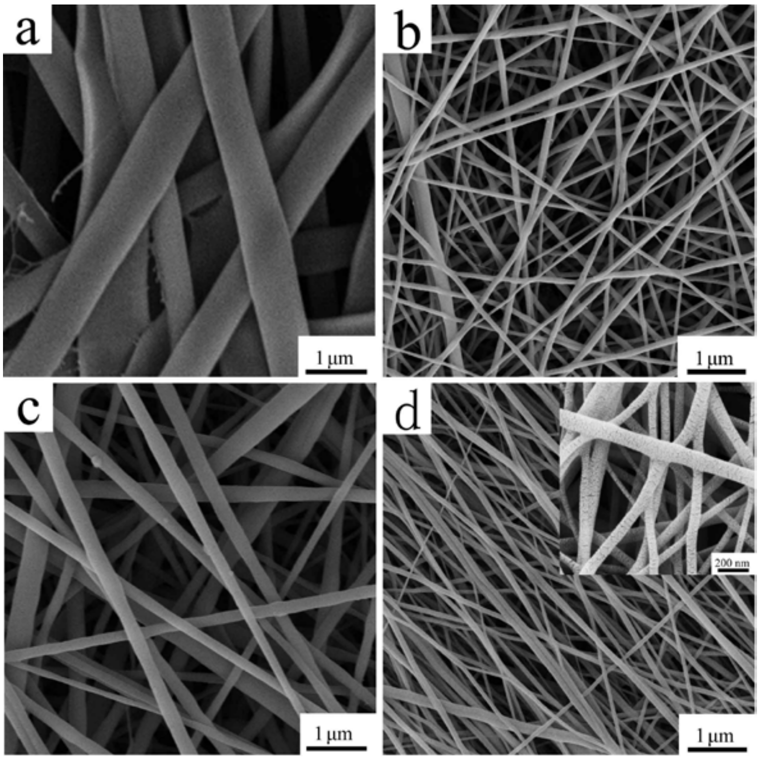

Fig. 4 SEM images of the fibrous membranes: (a) Nylon-6/PW, (b) Nylon-6/PMoV1, (c) Nylon-6/PMoV2, (d) Nylon-6/PMoV3; The inset in d is the corresponding high-magnification SEM image.

Fig. 4 shows the SEM images of four kinds of Nylon-6/POMs nanofibrous membranes. Fig. 4a corresponds to Nylon-6/PW nanofibrous membrane and the diameter of the nanofibers is 500~700 nm with a narrow size distribution. The SEM images of Nylon-6/PMoV1, Nylon-6/PMoV2 and Nylon-6/PMoV3 nanofibers were shown in Fig. 4b-d. It can be seen that the diameter of the Nylon-6/PMoVn nanofibers is ranging from 50 to 100 nm, which is much thinner than that of Nylon-6/PW nanofibers. During the preparation of the electrospinning sols, PW is more difficult to dissolve in formic acid comparing to others. If the solution was aged at room temperature, precipitate was easily formed in the Nylon-6/PW precursor solution. So the Nylon-6/PW precursor solution exhibited higher viscosity than the others, which led to the larger diameter of the electrospun fibers. In addition, the electrospinning system is an open system and the viscosity of the precursor solution increases as the solvent evaporation during electrospinning process, leading to the gradual increase of the fibers' diameter. In addition, orientation of the fibers was observed in Fig. 4d, which might be due to the momentary static electronic non-uniformity or the effect of the local wind force during the electrospinning.[36] Overall, the fibers exhibit thin diameter, which corresponds high specific surface area and favors their application in catalysis and adsorption.

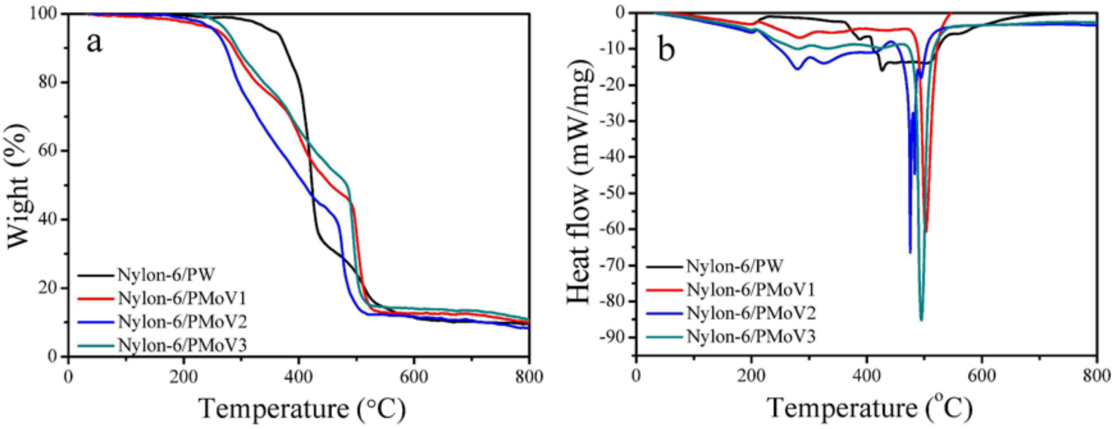

Fig. 5 TG (a) and DSC (b) curves of the fibrous membranes.

The thermal gravimetric and differential scanning calorimetric (TG-DSC) curves of Nylon-6/POMs nanofibrous membranes, obtained at a heating rate of 10 °C/min under air atmosphere, are shown in Fig. 5. The trace amount of mass loss (ca.2%) below 210 °C may be due to the removal of the residual solvent in the composite nanofibrous membranes, and no obvious endo/exothermic effect can be observed from the DSC curve. The weight loss from 210 to 520 °C should be ascribed to the decomposition of nylon-6 and POMs. There is an obvious exothermic peak in the DSC curve, which should be attributed to the decomposition and oxidation of nylon-6 and decomposition of POMs.[37] Due to the serious overlap of the decomposition of nylon-6 and POMs, it is difficult to identify them from the TG-DSC curves, but the result revealed that all the Nylon-6/POMs nanofibrous membranes have good thermal stability, which can be used below 200 °C safely.

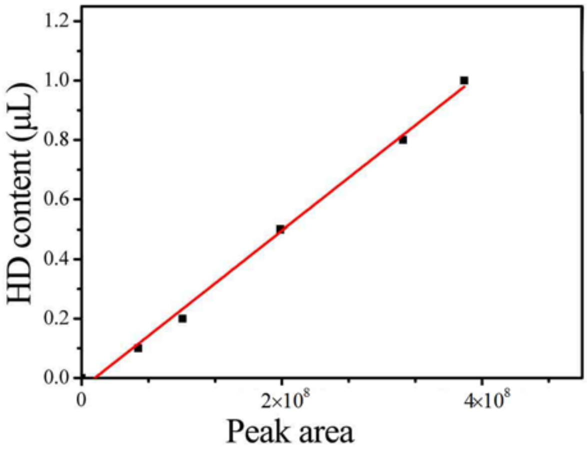

Fig. 6 Standard curve of HD solution.

The external standard method was used to detect the concentration of HD with degradation. First of all, HD standard curve was plotted. As shown in Table S1, a certain amount of HD standard solution and CH_2Cl_2 were mixed to obtain a series of HD solutions in which HD absolute content were 0, 0.1, 0.2, 0.5, 0.8, 1.0 μL, respectively. Then GC-MS was used to analyze the solutions, and the peak area of HD (Table S1) was obtained by integrating. Based on the peak area and the HD content, the standard curve shown in Fig. 6 was established. The equation of the standard curve is $y=2.65\times10^{-9}\times x - 0.34\times10^{-2}$. The correlation coefficient of the standard curve is 0.996, indicating the good linear correlation of the data, and the curve can be used to obtain accurate HD concentration.

Fig. 7 shows the degradation rate of HD as a function of degradation time in presence of the prepared Nylon-6/POMs nanofibrous membranes. It can be seen that Nylon-6/PMoV3 nanofibrous membrane exhibited superior property than the three others. Degradation rate of HD by Nylon-6/PMoV3 nanofibrous membrane was up to 41.55% in 6 h. The degradation rates of HD by the four kinds of nanofibrous membranes were in following order: Nylon-6/PMoV3 > Nylon-6/PMoV2 > Nylon-6/PW > Nylon-6/PMoV1. It is known that the addition of vanadium is beneficial for redox catalysis, shifting its reactivity from acid-dominated to redox-dominated, as demonstrated by the oxidation of some organic compounds,[38] and the substitution of Mo^{6+} with V^{5+} would result in the generation of more reactive lattice oxygen associated to the Mo–O–V species.[5,39] Therefore, the degradation ability of the POMs toward HD increased with the V content increasing. In addition, it is easier for PMoV1 to lose the crystallization water comparing to the other three POMs (Fig. 2). Although the Keggin anions can retain their mobility even in their dehydrated form, the lost of the water should affect their mobility to some extent,[40] which might result in the relative lower degradation ability of Nylon-6/PMoV1 nanofibrous membrane.

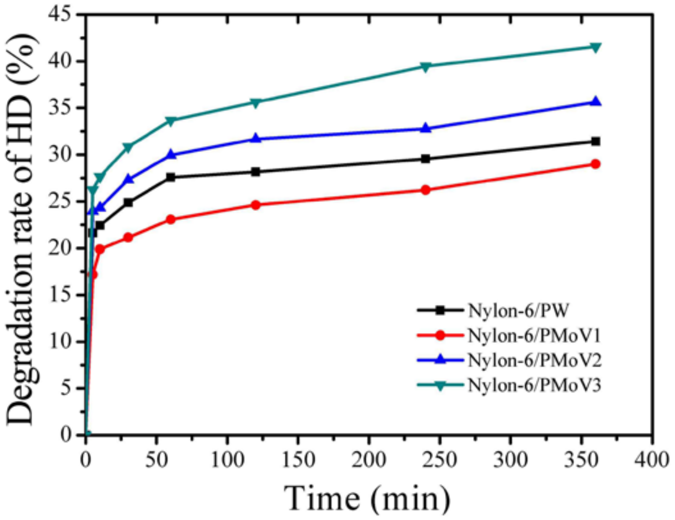

Fig. 7 Degradation of HD on Nylon-6/POMs nanofibrous membranes.

Table 2 Filtration efficiency and pressure drop for Nylon-6/PMoV3 fibrous membranes.

Sample	Electrospinning time (h)	Basic weight (g/m^2)	Pressure drop (Pa)	Aerosol filtration efficiency (%)
1	0	0	1.5	11.45
2	2	0.31	217	77.25
3	3	0.40	484	98.35

It is known that HD exists as aerosol at ambient condition, so it also can be blocked by filtration. Then, the filtration property of the composite nanofibrous membrane was evaluated. To evaluate aerosol filtration performance of nanofibrous membranes, a piece of PP nonwoven fabric was used as substrate to receive and support the Nylon-6/POMs nanofibrous membrane using Nylon-6/PMoV3 nanofibrous membrane as a typical example. Table 2 shows the filtration efficiency, pressure drop and basic weight of nonwoven fabric combined Nylon-6/PMoV3 nanofibrous membranes and the bare nonwoven fabric. It can be seen that aerosol filtration efficiency for PP nonwoven fabric was only 11.45%. As electrospinning time prolongs, aerosol filtration efficiency for samples significantly increases, and that of the 3 h electrospun nanofibrous membrane was up to 98.35%. In addition, the pressure drop for sample 3 was only 484 Pa. For this sample, the basic weight is 0.40 g/m^2, that is, the mass of per square meter Nylon-6/PMoV3 fibrous membrane is about 2.6 times of that used in the typical HD degradation experiment. The results showed that the as-prepared Nylon-6/PMoV3 nanofibrous membranes had excellent aerosol filtration performance and degradation property toward HD. It can be presumed that if the HD aerosol contacts with the composite nanofibrous membrane, most of the HD can be blocked by the membrane, and the few penetrated HD can be degraded rapidly.

In previous reports, the degradation of HD has been extensively studied, in which catalyst was supported on nanomaterials to degrade HD, such as TiO_2, activated carbon, and so on. They showed degradation ability to HD, but they could not be applied in protecting cloth due to the powder form of the supporting materials. The results revealed that the composite nanofibrous membranes have dual functions including degradation toward HD and filtration of aerosol, which shows potential application in protecting cloth with in situ degradation ability toward HD.

4. Conclusions

In summary, a novel flexible nanofibrous membrane containing POMs and nylon-6 has been successfully fabricated by electrospinning the mixed solution of nylon-6 and POMs. This composite nanofibrous membrane exhibited good performance to degrade HD. The degradation rate of HD on Nylon-6/PMoV3 nanofibrous membranes reached 41.55% in 6 h. At the same time, the membrane shows good filtration performance toward aerosol. Therefore, the composite nanofibrous membranes show potential application as a protecting cloth with the function of in situ degrading HD.

Acknowledgements

This work is supported by the Key Projects in the Science & Technology Pillar Program of China (No.2011BAZ02490) and the Natural Science Foundation of Shandong Province (ZR2011BZ002).

The authors thank Dr. Xiaobing Yang and Songtao Ding of State Key Laboratory of NBC Protection for Civilian, Beijing 100191, P. R. China for the help in the filtration and degradation characterization of the membrane.

References

1 Y. Yang, *Chem. Ind.*, 1995, **9**, 334-337.

2 Y. Yang, J. Baker and J. Ward, *Chem. Rev.*, 1992, **92**, 1729-1743.

3 A. Vorontsov, L. Davydov, E. Reddy, C. Lion, E. Savinova and P. Smirniotis, *New J. Chem.*, 2002, **26**, 732-744.

4 L. Bromberg, H. Schreuder-Gibson, W. Creasy, D. McGarvey, R. Fry and T. Hatton, *Ind. Eng. Chem. Res.*, 2009, **48**, 1650-1659.

5 A. Sharma, B. Singh and A. Saxena, *Carbon*, 2009, **47**, 1911-1915.

6 H. Liu and E. Iglesia, *J. Catal.*, 2004, **223**, 161-169.

7 M. Vazylyev, S. Dorit, A. Haimov, G. Maayan and R. Neumann, *Top. Catal.*, 2005, **34**, 93-99.

8 C. Hill, *J. Mol. Catal. A. Chem.*, 2007, **262**, 2-6.

9 D. Erik, *Rev. Med. Virol.*, 2000, **10**, 255-277.

10 D. Erik, *Med. Res. Rev.*, 2002, **22**, 531-565.

11 C. Hill, *Chem. Rev.*, 1998, **98**, 327-357.

12 M. Pope and A. Muller, *Angew. Chem. Int. Ed. Engl.*, 1991, **30**, 34-48.

13 Z. Xi, N. Zhou, Y. Sun and K. Li, *Science*, 2001, **292**, 1139-1141.

14 (a) K. Kamata, K. Yonehara, Y. Sumida, K. Yamaguchi, S. Hikichi and N. Mizuno, *Science*, 2003, **300**, 964-966. (b) N. Mizuno, C. Nozaki, I. Kiyoto and M. Misono, *J. Am. Chem. Soc.*, 1998, **120**, 9267-9272.

15 A. Hiskia, A. Mylonas and E. Papaconstantinou, *Chem. Soc. Rev.*, 2001, **30**, 62-69.

16 P. Lei, C. Chen, J. Yang, W. Ma, J. Zhao and L. Zang, *Environ. Sci. Technol.*, 2005, **39**, 8466-8474.

17 R. Johnson and C. Hill, *J. Appl. Toxicol.*, 1999, **19**, S71-S75.

18 C. Hill and R. Gall, *J. Mol. Catal. A. Chem.*, 1996, **114**, 103-111.

19 R. Gall, C. Hill and J. Walker, *J. Catal.*, 1996, **159**, 473-476.

20 K. Wu, P. Yu, C. Yang, G. Wang and C. Chao, *Polym. Degrad. Stab*., 2009, **94**, 2170-2177.

21 A. Saxena, A. Srivastava, B. Singh and A. Goyal, *J. Hazard. Mater*., 2012, **211**, 226-232.

22 B. Singh, A. Saxena, A. Nigam, K. Ganesan and P. Pandey, *J. Hazard. Mater*., 2009, **161**, 933-940.

23 M. Naseri, M. Sarabadani, D. Ashrafi, H. Saeidian and M. Babri, *Environ. Sci. Pollut. Res*., 2013, **20**, 907-916.

24 R. Ozer and J. Ferry, *J. Phys. Chem. B*, 2002, **106**, 4336-4342.

25 J. C. Edwards, C. Y. Thiel, B. Benac and J. F. Knifton, *Catal. Lett.*, 1998, **51**, 77-83.

26 J. Alcaniz-Monge, G. Trautwein, S. Parres-Esclapez and J. Macia-Agullo, *Micropor. Mesopor. Mater*., 2008, **115**, 440-446.

27 R. Gall, C. Hill and J. Walker, *Chem. Mater.*, 1996, **8**, 2523-2527.

28 M. Gorji, A. Jeddi and A. Gharehaghaji, *J. Appl. Polym. Sci.*, 2012, **125**, 4135-4141.

29 J. Y. Lin, X. F. Wang, B. Ding, J. Y. Yu, G. Sun and M. R. Wang, *Critical Reviews in Solid State and Materials Sciences*, 2012, **37**, 94-114.

30 X. F. Wang, B. Ding, G. Sun, M. R. Wang and J. Y. Yu, *Prog. Mater. Sci.*, 2013, **58**, 1173-1243.

31 J. Deitzel, J. Kleinmeyer, D. Harris and T. Beck, *Polymer*, 2001, **42**, 261-272.

32 Y. Kang, C. Park, C. Kim and T. Kang, *Fibers and Polymers*, 2007, **8**, 564-570.

33 H. Pant, M. Bajgai, K. Nam, Y. Seo, D. Pandeya, S. Hong and H. Kim, *J. Hazard. Mater.*, 2011, **185**, 124-130.

34 I. Kozhevnikov, *Chem. Rev.*, 1998, **98**, 171-198.

35 A. Bielanski, A. Malecka and L. Kybelkova, *J. Chem. Soc. Faraday Trans.*, 1989, **85**, 2847-2856.

36 (a) A. Theron, E. Zussman and A. L. Yarin, *Nanotechnology*, 2001, **12**, 384-390; (b) H. Fong, W. D. Liu, C. S. Wang and R. A. Vaia, *Polymer*, 2002, **43**, 775-780; (c) D. Li, Y. Wang and Y. Xia, *Adv. Mater.*, 2004, **16**, 361-366.

37 P. Z. Wang, J. Y. Niu, L. Xu, J. Peng and E. B. Wang, *Acta Chim. Sinica*, 1995, **53**, 757-764.

38 J. Y. Wang, C. W. Hu, M. Jian, J. Zhang and G. Y. Li, *J. Catal.*, 2006, **240**, 23–30.

39 M. Akimoto, H. Ikeda, A. Okabe and E. Echigoya, *J. Catal.*, 1984, **89**, 196-208.

40 M. Misono, *Catal. Rev. Sci. Eng.*, 1987, **29**, 269-321.